ORIGINAL PAPER-EXPLORATION ENGINEERING

PDC bit optimization scheme for tight oil reservoirs in the Jidong Oilfield based on rock anti-drilling characteristics

Xu Xiaofeng[1] · Song Wei[1] · Zhu Kuanliang[1] · Wang Changhao[2] · Zhou Yan[1] · Li Yunfeng[1] · Li Shibin[2]

Abstract

The tight oil reservoir rocks in the Jidong Oilfield are generally characterized by high hardness, strong abrasiveness, and extremely unevenness, which seriously reduce the drilling efficiency. In view of this problem, the mineral composition, hardness, plasticity coefficient, and drillability of rocks were first determined. It was found that the rock integrity, compactness and high hardness are the main factors leading to the low rock breaking efficiency of PDC bits. Then, combined with logging data, the drilling resistance profile of the whole well section was established. According to the crushing mechanism of rocks under the action of a PDC bit, the mechanical model of a single composite plate under rock crushing conditions is established, and the influence of the back angle on the cutting force is analyzed. The flow field distribution of the drill bit surface under different nozzle combinations was calculated by finite element numerical simulation. Based on the experimental and simulation results, the optimal backward angle was 15°, and the optimal nozzle combination was two 16-mm central nozzles and five 14-mm peripheral nozzles. Finally, a personalized PDC bit design scheme for tight oil reservoirs in the Jidong Oilfield was proposed. The scheme includes the following: (1) a 5-blade straight-arc crown is profiled; (2) anti-impact cylindrical components are set; (3) the nozzle hydraulic structure adopts a bending type; and (4) the diameter-retaining teeth and diversion grooves are optimized. The optimized bit reduces stick–slip, improves stability, and has an obvious acceleration effect.

Keywords PDC bit · Tight oil · Drillability · Drilling speed increase · Rock fragmentation

Introduction

The deep tight oil reservoir in the Jidong Oilfield has the characteristics of high hardness, poor drillability, and extreme heterogeneity, and it is difficult for bits to penetrate into the formation (Haimin et al. 2006; Li et al. 2021; Xisheng 2009). The bit is the most important rock-breaking tool in the drilling process. Only when the selected bit type has good compatibility with the drilled formation can the drilling efficiency be greatly improved and the service life of the bit be increased.

At present, many scholars have performed much research on PDC bits breaking rocks. Geoffroy (Geoffroy and Minh

1997) analyzed the cutting process of composites under the combined action of axial forces and tangential forces. Prasad (Checkina et al. 1996) conducted cutting experiments of composite slices on rocks under different hydrostatic pressures and established a stress model of composite slices. Chen Yinghua (Chen 2008) analyzed the interaction between composites and rocks via experiments. In view of this formation, the penetration ability is continuously improved through the personalized design of the drill bit, but the effect of the speed increase is still not obvious, which seriously affects the production capacity construction and development process (Zhou et al. 2019). To solve the above problems, the causes of mismatch between the drill bit and formation should be analyzed. First, the mineral composition, hardness, and plasticity coefficient of the rock are tested, the PDC and drillability of the roller bit are tested, and the distribution profile of the drilling resistance characteristics in the whole well section is established. Then, by analyzing the interaction force between the bit and the formation, the optimal design scheme of the bit that is suitable for deep complex rock formations is proposed, which is of

✉ Wang Changhao
229166411@qq.com

1 Institute of Drilling and Production Technology, Petro China Jidong Oilfield Company, Tangshan 063000, Hebei Province, China

2 Northeast Petroleum University, Daqing 163318, Heilongjiang Province, China

great significance to ensure the continuous speed increase and cost reduction in the Jidong Oilfield. The research process of this paper is shown in Fig. 1.

Drilling resistance tests of rocks

This paper comprehensively evaluates the mineral composition and drilling resistance of deep tight oil reservoir rocks in the Gaoshangpu area of the Jidong Oilfield. The experimental cores are mainly the tight oil reservoirs in wells Gao 23–39 and Gao 23–74. The depth of the coring section is located between 3800 and 4300 m, and the core coverage is comprehensive. The core information is shown in Table 1.

Analysis of rock mineral compositions

X-ray diffraction (XRD) was used to analyze and test the mineral compositions of the core. According to the mineral diffraction pattern, the mineral compositions and contents of the rock samples were determined. This experiment refers to the petroleum and natural gas industry standard of the People's Republic of China: the X-ray diffraction analysis method of clay minerals and common nonclay minerals in sedimentary rocks (SY/T 5163-2018). The statistical analysis of the data and the results of the mineral composition analysis in the study area are shown in Fig. 2.

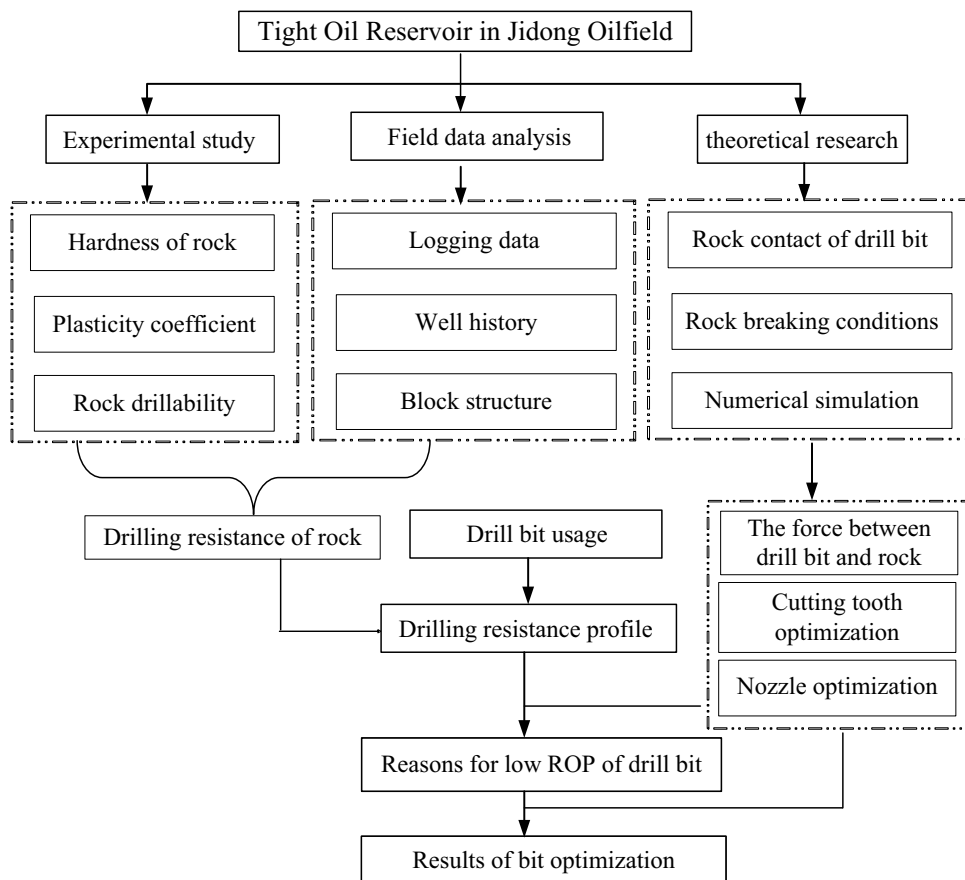**Fig. 1** Flow chart of the research process

Table 1 Core information

Core number	Well number	Depth (m)	Stratum horizon	Lithology
1	Gao 23–39	3800.67–3800.77	Es32+3	Gray argillaceous sandstone
2		3906.81–3907.00	Es32+3	Gray oil-bearing fine sandstone
3		3923.70–3923.91	Es32+3	Gray–brown oil-bearing fine sandstone
4	Gao 23–74	4227.42–4227.55	Es32+3	Gray mudstone
5		4234.45–4234.61	Es32+3	Light gray medium sandstone
6		4261.61–4261.8	Es32+3	Gray–brown oil-saturated medium sandstone
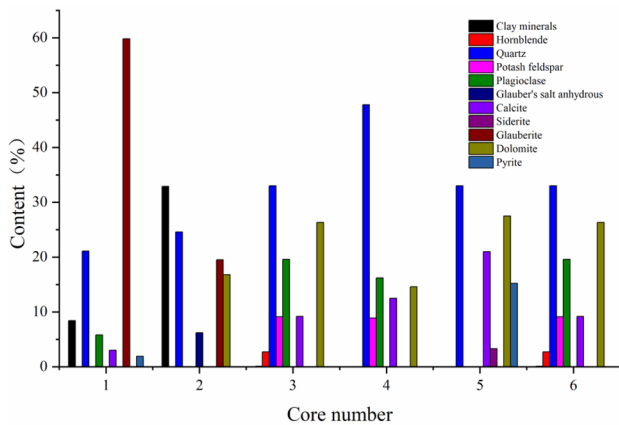
Fig. 2 Results of rock mineral grouping analysis

Fig. 3 The broken teeth

The main rock-forming minerals in the deep tight oil reservoirs of the Jidong Oilfield are widely distributed, in which quartz, plagioclase, and dolomite are abundant, and some rocks contain a large amount of clay. Quartz and other rock-forming minerals have the characteristics of high hardness and brittleness. It is difficult for the mineral particles to be broken by the drill bit. When the bottom hole cannot clean the cuttings in time, the broken particles cause serious wear to the drill bit (Wang et al. 2015).

Hardness and plasticity coefficient test

The hardness and plasticity coefficient of the core were tested by an automatic rock hardness tester. The rock sample was placed between the tray and the pressure head, and an axial load was applied until failure. The stress and strain curves were recorded, and the rock hardness and plasticity coefficient were calculated.

In the process of the experiment, the pressure head collapse phenomenon occurred many times, indicating that the hard mineral content in the rock is high, and the local indentation hardness is too large, resulting in the cemented carbide pressure head not being pressed into the rock and causing damage, as shown in Fig. 3.

The experimental results of the hardness and plasticity coefficient are shown in Table 2.

The rock hardnesses of deep strata in the Jidong Oilfield are quite different, indicating that the hardness has strong heterogeneity and anisotropy, and the hardness values are distributed between 340 and 1962 MPa, which generally indicates medium-soft to medium-hard strata. Some rocks reach a hard stratum of grade 7, and the pressure head is broken during the experiment. The plasticity coefficient is also quite different and is mainly distributed from 1 to 2. Under the condition of no confining pressure, the plasticity is generally low, and some rocks show strong brittleness in
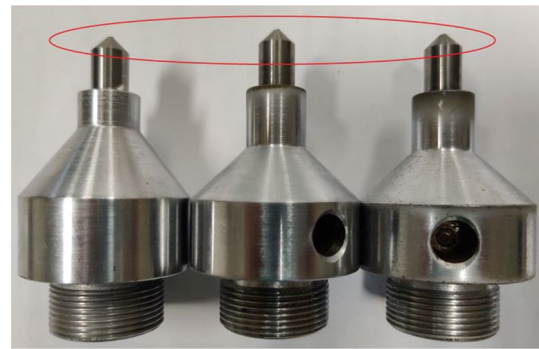
direct brittle fracture experiments. Some of the important reasons for the low ROP are the interlacement of soft and hard rocks, more medium to hard rocks, and strong heterogeneity (Arsentiev et al. 2018).

Rock drillability tests

The microdrilling rate experiment was used to determine the drillability level of rock via indoor PDC and roller microbit experiments. This experiment refers to the national standard of the People's Republic of China: the determination and classification of rock drillability in petroleum and natural gas drilling engineering (SY/T5426-2016). After the drillability grade value is obtained, the rock drillability grade standard contrast table is assessed and graded. Some experimental photos are shown in Fig. 4.

The drilling time is used to represent the degree of difficulty when the formation is broken. By a logarithmic transformation of drilling time T, the relationship between the rock drillability level of the cone bit and microdrilling time can be obtained:

$$K_d = \log_2 T \tag{1}$$

The calculation formula of the rock drillability level of the PDC bit is calculated by Formula (2) and Formula (3).

$$K_d = \log_2 T + G_i \tag{2}$$

$$G_i = 2^{i-1} - 1 \tag{3}$$

where K_d is the drillability level value; T is the drilling time, in s; G_i is the equivalent conversion level value; and i is the drilling pressure series (in the first stage, $G_i = 0$, in the second stage, $G_i = 1$, and in the third stage, $G_i = 3$).

The experimental results of rock drillability are shown in Table 3.

The PDC bit drillability grade values are mainly 6–10, and they are all difficult drilling formations with soft and hard staggering. Slippage occurs in some cores. All cores

Table 2 Test results of the hardness and plasticity coefficient

Core number	Hardness			Plasticity coefficient		
	Hardness/MPa	Grade	Class	Plasticity coefficient	Grade	Class
1	1149.68	5	Medium-hard	1.62	2	Low-plasticity
2	705.67	4	Medium-soft	1.51	2	Low-plasticity
3	610.52	4	Medium-soft	2.12	3	Medium-plasticity
4	872.17	4	Medium-soft	1.80	2	Low-plasticity
5	1617.48	6	Medium-hard	1.16	2	Low-plasticity
6	868.21	4	Medium-soft	1.14	2	Low-plasticity

Fig. 4 Rock photographs of the drillability experiment
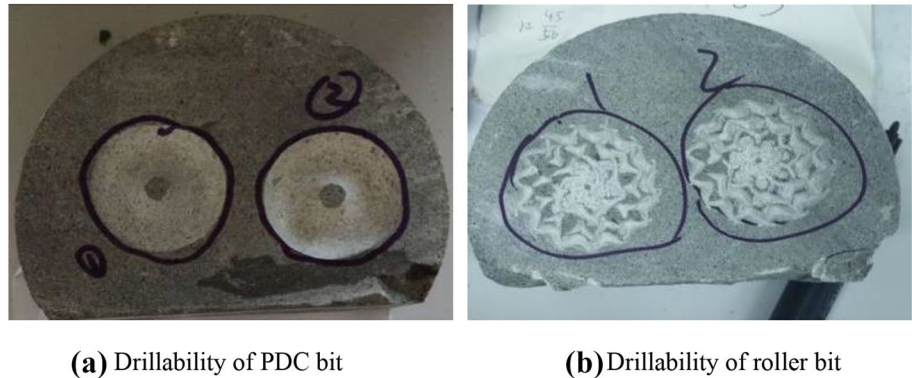
(a) Drillability of PDC bit   **(b)** Drillability of roller bit

Table 3 Rock drillability test results

Core number	PDC bit			Cone bit	
	Drilling pressure level	Drilling time/s	Drillability level	Drilling time/s	Drillability level
1	Level 3 (2KN)	20.3	7.34	140.8	7.12
2	Level 3 (2KN)	93	9.53	786.8	9.62
3	Level 3 (2KN)	12.2	6.61	100.7	6.65
4	Level 3 (2KN)	51.8	8.35	177.57	7.44
5	Level 3 (2KN)	Sliding	>10	1001.6	>10
6	Level 3 (2KN)	22	7.43	162.03	7.32

When some rock is drilled to a certain depth, the bit no longer gains footage, the failure surface becomes smooth, and this is known as sliding. When the drilling time is more than 128 s under tertiary drilling pressure, the drillability level is greater than 10

can be drilled only under three-level drilling pressure, indicating high rock hardness, and cutting teeth with low drilling pressure cannot effectively eat into the formation; thus, the rock cannot produce a large shear fracture volume (Wang 2019).

The drillability of the roller bit is mainly distributed in grades 6–10; it is primarily grade 7 and partially skids. This shows that the ability of bit teeth to press into the rock is poor and proves the high hardness of the rock.

Combined with the results of mineral composition analysis, the rock in this block is complete and dense, the particles are fine and dense, and the hardness is high. It is

difficult to shear the PDC bit to produce volume crushing, but only surface crushing or fatigue crushing can break the rock, resulting in extremely low efficiency (Ji et al. 2021).

Profile description of formation drilling resistance characteristics

Formation anti-drilling characteristics are the main basis for determining drilling methods, selecting rock breaking tools, predicting the ROP and optimizing drilling parameters. Starting from the formation anti-drilling characteristics, the above parameters, such as rock drillability, are measured,

and the correlation model between formation anti-drilling characteristic parameters and logging data is established by using mathematical statistics (Zhongfu et al. , 2006; Wangde et al. 2021). By sampling and measuring the anti-drilling characteristic parameters of deep cores in the Jidong Oilfield and with the help of existing drilling data (including logging data, well history data and core data), the distribution of anti-drilling characteristic parameters such as hardness and drillability along the longitudinal direction is studied, as shown in Fig. 5.

Using the drill-resistant characteristic chart, the formation hardness, drillability of cone bits, drillability of PDC bits, shale content, and lithology distribution corresponding to a deep well in the Jidong Oilfield can be directly searched. Figure 5 shows that the drillability of the PDC bit and roller bit in deep formations is very different, and the maximum is more than 10 grades. The prediction profile of formation anti-drilling characteristics can be used in combination with the recommended bit instructions provided by different bit manufacturers when the bit is out of the factory. The bit with poor compatibility with the formation is not even suitable for this formation, and it is not directly listed as the alternative bit in the bit selection scheme, avoiding the repeated work of the secondary selection, which can provide the basis for the bit selection (Tie et al. 2021).

Mechanical analysis of PDC bits breaking rocks

The drillability level of deep rock in the Jidong Oilfield is very high regardless of the PDC bit or roller bit, which is not conducive to breaking rocks by bit. However, since the main rock-breaking method of the cone bit is crushing by pressing, while the PDC bit is a cutting bit, the cutting tooth has the advantage of self-sharpening. When crushing the rock, there is no holding effect of the cone bit, and the cutting area is larger, so it is an efficient bit (Yahiaoui et al. 2013). A greater benefit can be obtained when the PDC bit is adapted to the formation. Therefore, to improve the bit feeding ability of deep rock in the Jidong Oilfield to thereby improve the ROP, this paper mainly analyzes the interaction process between the PDC bit and rock formation and establishes a mechanical model of the formation-PDC bit system under rock crushing conditions.

Force of the single tooth composite sheet PDC

Assuming that the axial and horizontal loads acting on a single PDC piece by a rigid bit are F_{PN} and F_{PS}, respectively, the theoretical model (Wang et al. 2019) is shown in Fig. 6. α is the back rake angle of the cutting tooth; F'_{PN} is the reaction force of rock on the composite sheet when a single composite sheet is vertically pressed into the rock at a certain depth d, so $F'_{PN} = F_{PN}$; F'_{PS} is the reaction force of the rock to the
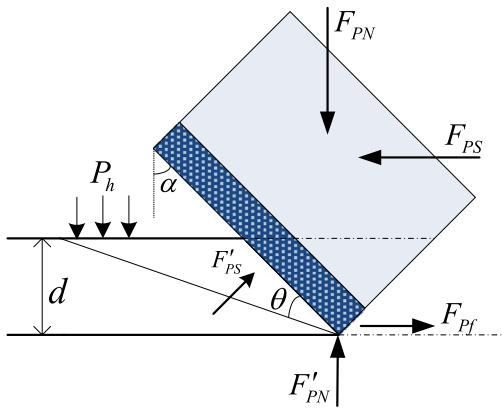

Fig. 5 Drilling resistance profile of well G32-P2
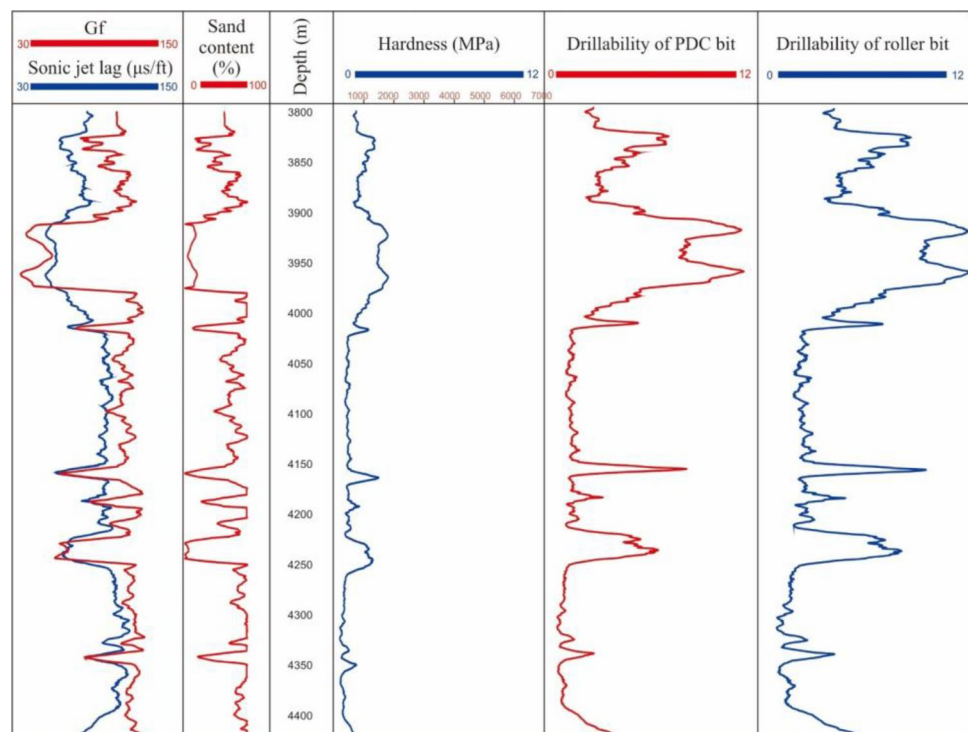
Fig. 6 Cutting process of the composite sheet

composite plate when the limit displacement of the composite plate reaches the requirement of broken rock; and F_{Pf} is the horizontal friction between the bottom of the composite sheet and the rock. Under the bottom hole condition, the free surface of the rock is also subjected to a uniform distribution of pressure P_h, which is the difference between wellbore pressure and formation pressure. As shown in Fig. 7, the unit body of the cut rock and its symmetrical surface are extracted for analysis. The bottom hole pressure difference acts on the free surface ABEF, and its surface area is S_{P1}. Therefore, the uniformly distributed pressure can be simplified to the concentrated force $F_{P3} = P_h \cdot S_{P1}$. The area of the rock shear plane ABCD is S_{P2}, and the shear failure angle is θ. The shear surface is subjected to normal stress σ_n and shear stress τ. The contact normal stress and friction resistance are distributed on the CDFE of the contact surface between the cutting tooth and the rock unit. The friction angle is set as β, and the resultant force is F_{P2}.

The normal stress σ_n and shear stress τ on the shear plane are as follows:

$$\sigma_n = (b + 1)\frac{\sin\theta}{d}\sin(\alpha + \beta + \theta)F_{P1} \tag{4}$$

$$\tau = (b + 1)\frac{\sin\theta}{d}\cos(\alpha + \beta + \theta)F_{P1} \tag{5}$$

According to the Mohr–Coulomb criterion, the resultant force on the shear fracture surface ABCD is:

$$F_{P1} = \frac{c \cdot S_{P2}}{(b + 1)\sin\theta\cos(\alpha + \beta + \varphi + \theta)} \tag{6}$$

The shear fracture angle can also be obtained by the extreme value of the above formula:

$$\theta = \frac{\pi}{4} - \frac{\alpha + \beta + \varphi}{2} \tag{7}$$

The forces on the unit body are simplified as the concentrated forces in the symmetric plane of the unit body (Sinor et al. 1998). According to the force balance conditions in the X- and Y-directions, there are:
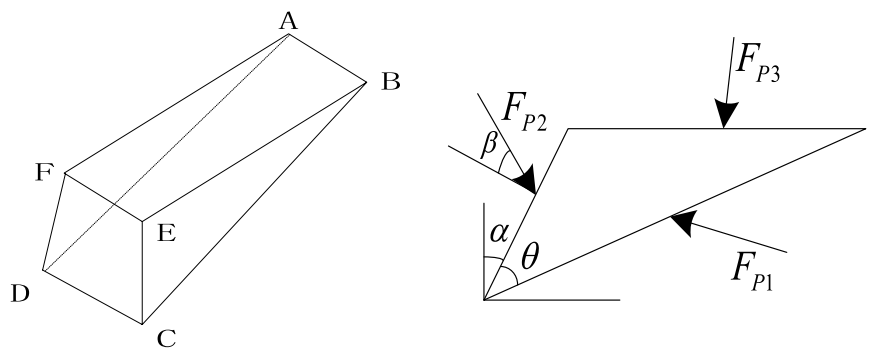
$$\sum X = 0 : F_{P2}\sin\left(\frac{\pi}{2} - \alpha - \theta - \beta\right) - F_{P1}\cos\beta - F_{P3}\sin\theta \tag{8}$$

$$\sum Y = 0 : F_{P1}\sin\beta - F_{P2}\cos\left(\frac{\pi}{2} - \alpha - \theta - \beta\right) - F_{P3}\cos\theta \tag{9}$$

The force between the working face of the cutting tooth and the rock before the cutting edge is:

$$F_{P2} = \frac{cS_{P2}}{(b + 1)\sin\theta\cos(\alpha + \beta + \varphi + \theta)} + \frac{P_h S_{P1}(\cot\theta - \tan\alpha)\sin(\varphi + \theta)}{\cos(\alpha + \beta + \varphi + \theta)} \tag{10}$$

Fig. 7 Stress analysis of the rock mass


(a) Unit of cut rock

(b) Force on the symmetrical surface of the unit

Effect of the back angle of the composite sheet on the cutting force

The back angle of the cutting tooth is an important design parameter of the PDC drill bit. Sinor (Kuang et al. 2016) used a different rear angle of the cutting tooth in a variety of rock-like cutting tests. The PDC cutting teeth are minimal when the back angle is close to 10°, and the rotational torque is also minimized. As the angle increases, the cutting teeth, axial force, and torque increase.

In the stress analysis of the PDC composite plate, the mechanical model of rock breaking by a single tooth composite plate is established, and the parameters of the back angle are included in the model. Therefore, the rock mechanical parameters are substituted into the model to analyze the variation in the axial force and tangential force on the cutting tooth when the dip angle changes from 5 to 30°, as shown in Fig. 8.

As shown by the calculation results, as the angle increases, the axial force is constantly increasing and gradually tends to be smooth. The tangent force increases, and a significant turning point occurs. Since the rock hardness of the study block is generally high, some rocks reach 7, and turbulence occurs many times during the experiment. The PDC bit and roller bit often slip on the rock surface because of the rock hardness, so that the cutting teeth cannot be effectively pressed into the formation. Therefore, only the axial force can avoid slipping with the cutting teeth. At the same time, it is understood from Formula (10) that the shear destructive angle increases when the tangent force increases, and the larger rock volume of the cutting tooth increases. However, the axial force and tangential force cause the composite sheet to be prematurely damaged and reduce the life of the drill bit. For the above two reasons, the most suitable rear angle is determined by the relationship between the rear inclination angle and the cutting tooth.
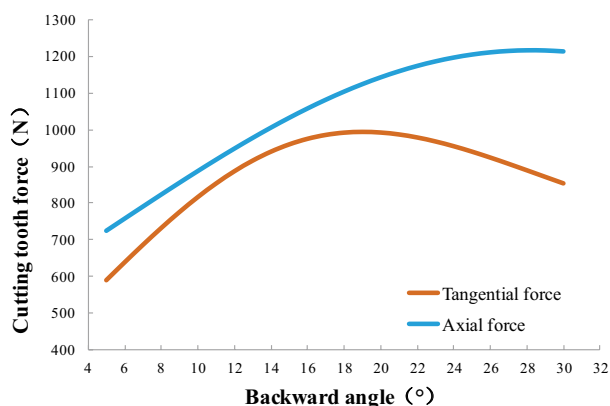
When the caster angle reaches 10°, the growth rate of the tangential force and axial force reaches the maximum. When the angle is increased again, the cutting force gradually stabilizes, and the tangential force reaches the maximum when the caster angle reaches 18°. The axial force reaches the maximum when the caster angle reaches 25°, but the tangential force is significantly reduced at this time. Therefore, when the back inclination angle of the cutting teeth of the drill bit is designed to be 15–20°, a large stress concentration can be generated on the tooth edge and cutting surface so that the cutting teeth can cut into the formation more easily, which is beneficial to the cutting teeth in shearing rock and improves the efficiency of rock breaking.

Bit optimization of tight oil reservoirs

Based on the indoor drilling resistance tests and field drilling analyses, the main reasons for the slow drilling speed of deep formations in the Jidong Oilfield are as follows:

① There are many interlayers, and the formation is soft and hard. The adaptability of the drill bit to the formation becomes more difficult. The PDC is prone to slippage in the rock microdrilling experiment. ② The mud content of some rocks is high, and the drill bit easily packs mud. ③ The drilled stratum has a large number of cuttings after the rock is broken, and there are more clay minerals, making the bottom hole more difficult. ④ Existing drill bits have certain defects in the cutting tooth structure and nozzle size, resulting in insufficient aggressiveness of the composite sheet, and it is not easy to cut into the ground and cause slipping.

Therefore, in view of the above problems, numerical simulation is used to analyze the rock breaking effect of the drill to give the optimal geometric parameters, such as the cutting tooth inclination angle and the nozzle combination.

Optimization of the back angle of the cutting teeth

(1) Material parameters

The rock density is 2.5 g/cm^3, the elastic modulus is 27.6 GPa, and Poisson's ratio is 0.23. The Drucker–Prager plasticity criterion was adopted, where the internal friction angle is 53°, the flow stress ratio is 0.8, the dilatancy angle is 10°, and the ultimate strength in the hardening criterion is 150 MPa. The density of the cutting tooth is 7.85 g/cm^3, the elastic modulus is 210 GPa, and Poisson's ratio is 0.3.

(2) Load infliction

A boundary load is applied to the cutting tooth of the drill bit, where the drilling speed is 2 mm/s, the speed is 2 rad/s, and the lateral and bottom of the rock are fixed constraints.

Fig. 8 Relationship between the force of the cutting teeth and inclination angle

In addition, surface contact is adopted between the cutting tooth and the rock; that is, surface-node contact is carried out between the surface of the cutting tooth and the rock grid node, which is convenient for generating new contact after continuously breaking the rock.

The simulation model of PDC single tooth cutting is established, and a fixed horizontal load is loaded on the chip tooth (Zhenquan and Dongyu 2014). Then, four representative different dip angles are selected to analyze the rock breaking effect of the cutting tooth: 5–20°. The cutting effect of different inclination angles is compared. From the simulation results, the rock breaking force effect of cutting teeth under different inclination angles is revealed, as shown in Fig. 9.

When the back angle of the cutting tooth is 5°, the maximum stress is concentrated in a small range of strata at the front of the cutting tooth. With the increase in the back angle, the stress and the range of stress action also increase. When the back angle of the cutting tooth is 15°, the cutting

tooth acts on the inner side of the rock stratum with large stress, resulting in a wide range of large stress areas. However, when the dip angle continues to increase, the stress range changes little. This shows that although the increase in the back rake angle can increase the ability of the single tooth of the drill bit to press into the formation, there is an upper limit. After the back rake angle is increased to the upper limit, the cutting force remains unchanged. Therefore, for this research formation, the rock breaking effect is the best when the back rake angle is 15°. This is also consistent with the conclusion of the relationship between the force and the back angle of the PDC composite analyzed in Sect. 3.2.

Optimization of PDC bit nozzle size

(1) Model establishment and grid division
   The actual bit is imported into fluent software for flow field establishment and Boolean operation. The

(a) 5° inclination angle

(b) 10° inclination angle

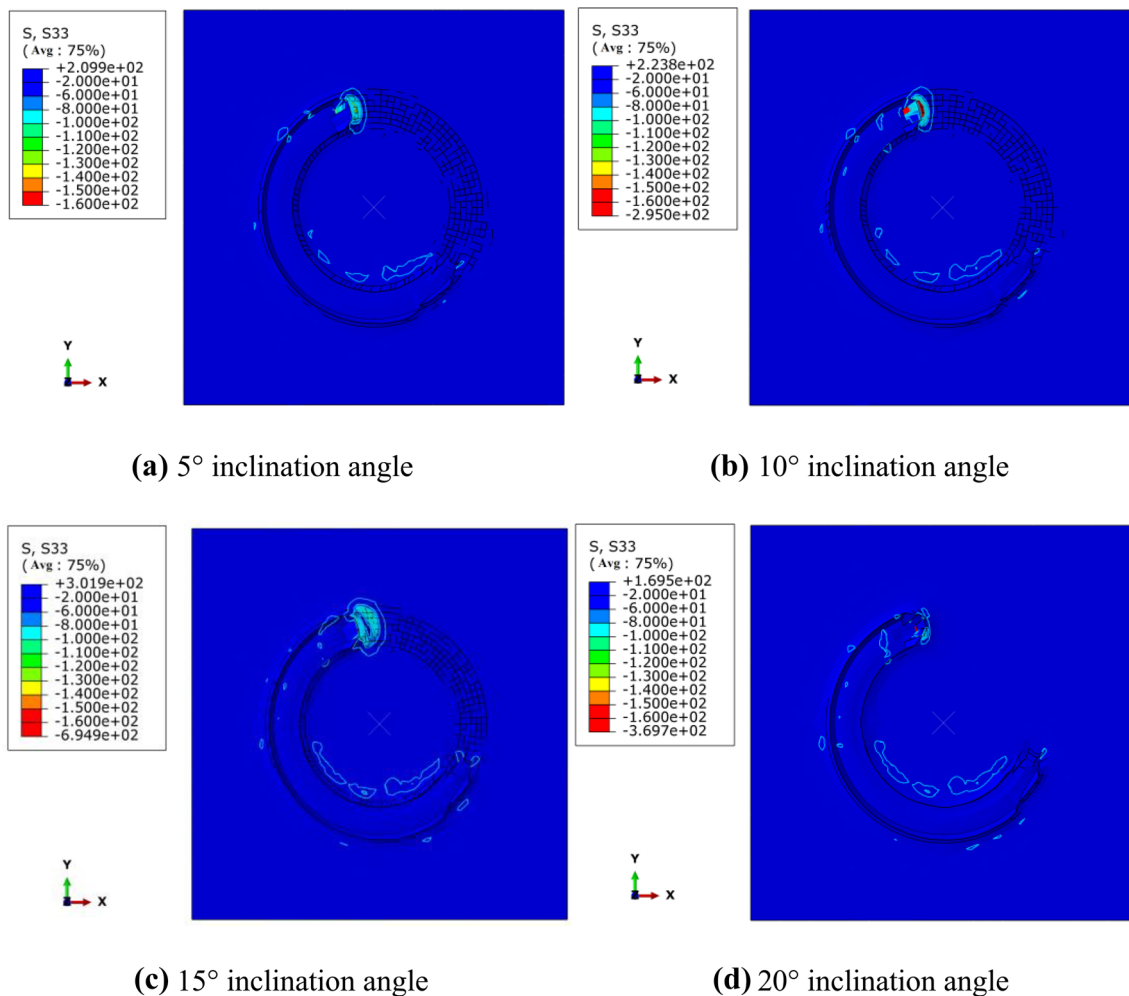**(c)** 15° inclination angle

(d) 20° inclination angle

Fig. 9 Cutting effect of different back angles

solid domain and internal and external fluid domains of the bit are removed. The tetrahedral mesh is used for meshing, and the mesh size is 2 e–3 m, which ensures the accuracy of the calculation.

(2) Model selection and boundary settings

The bit has jet and lateral flow in the bottom hole flow field, so its environment is in a turbulent flow field. The transient analysis is adopted here. The turbulence model adopts k-ε. The fluid uses water as the computational fluid. The inlet is the velocity inlet, which is 2 m/s. The outlet is the pressure outlet, which is the free flow outlet, and the calculation time is 10 s.

The numerical analysis and optimization design of the nozzle flow field are carried out by using the 5-blade PDC provided by the drill. First, two different nozzle combinations are set up; from the center to the periphery, the sizes are: ① 2×14 mm $+ 5 \times 16$ mm, and ② 2×16 mm $+ 5 \times 14$ mm. In the first combination, the diameter of the central nozzle is smaller than that of the peripheral nozzle, and the stage difference is $- 2$ mm. In the second combination, the diameter of the central nozzle is larger than that of the peripheral nozzle, and the difference is 2 mm. Numerical simulation of the flow field and pressure field of the two groups of nozzles is carried out, and the fluid-assisted rock breaking and bottom hole cleaning effect are analyzed in two cases. The simulation results are shown in Fig. 10.

The above simulation results reveal that the jet velocities of the two sets of nozzles are 19.83 m/s and 21.86 m/s, respectively, as shown in Fig. 10a. The fluid sprayed by the first group of nozzles does not form good coverage on the main blade, which is not conducive to lubricating the drill bit composite sheet; the second group of nozzles can form a diffuse flow field from the center to the well wall at the bottom of the drill bit. The fluid in the flow field more fully covers the blades and diversion grooves and has a good flow thrust to remove bottom hole cuttings and cool the bit, as shown in Fig. 10b. In addition, the first group of fluids has a strong impact on the drill bit composite sheet, and the cutting teeth have a stress concentration phenomenon, which shortens the service life of the drill bit. The second group of fluids acts evenly on the surface of the bit, and the severity of local erosion on the surface of the bit and the teeth is decreasing, indicating that increasing the size of the internal nozzle has a good anti-erosion effect, as shown in Fig. 10c.

To obtain a reasonable nozzle size, three different nozzle combinations are designed for simulation: ③ 2×18 mm $+ 5 \times 12$ mm; ④ 2×17 mm $+ 5 \times 13$ mm; and ⑤ 1×16 mm $+ 1 \times 18 +$ mm $+ 5 \times 13$ mm. The fifth group consists of two center nozzles with different diameters. The simulation results are shown in Fig. 11.

According to the simulation results, the maximum flow velocities of the second to the fifth groups are 21.86 m/s,

23.96 m/s, 23.20 m/s, and 23.21 m/s, respectively, and there is little difference in the velocity field. In terms of the area covered by the flow field, both the fourth and fifth groups produce a vortex zone at the center of the drill bit (Liu et al. 2018). In terms of the area covered by the flow field, both the fourth and fifth groups have a vortex zone at the center of the bit. This is because the high-speed fluid ejected from the nozzle exchanges momentum with the existing downhole submerged fluid. This causes the boundary layer to thicken continuously and then form an overflow. The overflow in the radial direction is forced to turn to the outlet due to the restriction of the borehole wall, which drives the movement of the submerged fluid in the process. The submerged fluid also forms a vortex area due to the unbalanced force in the incident and outflow directions. The vortex area has a huge impact on the flow field and the cuttings carried by the fluid. The cuttings in the vortex area continue to scour the bit and reduce the life of the bit (Yang et al. 2012). In the third group of spray combinations, although there is no vortex zone, there is no streamline passing through the crown of the main blade, indicating that this position cannot be well lubricated by the drilling fluid. The small diameter difference between the central nozzle and the peripheral nozzle leads to a decrease in the flow velocity at the outlet center of the central nozzle and that at the outlet center of the peripheral nozzle. The size of the central nozzle is larger than that of the peripheral nozzle to produce better auxiliary rock breaking and protection of the drill. Based on the above five sets of simulation results, the nozzle diameter combination of the second set is most conducive to the cooling, lubrication, and bottom hole cleaning of the drill bit. That is, it is most reasonable to design two 16-mm central nozzles and five 14-mm peripheral nozzles.

Overall optimization plan

The drill bits that can effectively break deep tight oil reservoirs in the Jidong Oilfield should have the following characteristics: ① strong wear resistance; ② strong impact resistance; ③ counter-cone milling into rock mass; and ④ effective cleaning of the bottom hole to prevent repeated wear of cuttings on the drill bit. Therefore, the overall bit optimization scheme is proposed as follows:

(1) Five drill blades are designed, and the straight-arc conical crown section is selected as the crown section shape.

(2) Two shock-resistant cylindrical parts are arranged on the same shoulder and elbow part of each blade wing of the crown of the drill bit, and a spring structure is arranged inside the part. If the drill bit encounters a hard formation or is used with a vibrating hammer and other drilling tools, reciprocating motions such as cut-
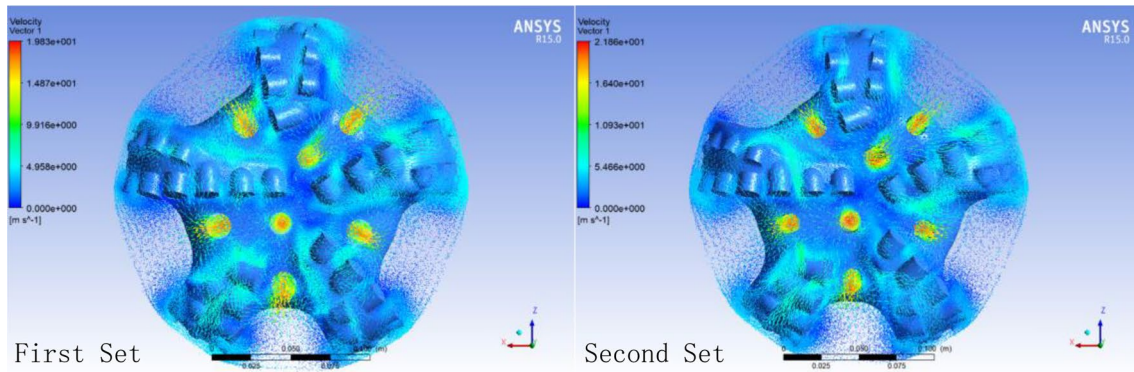
(a) Contrast cloud map of the fluid velocity field distribution
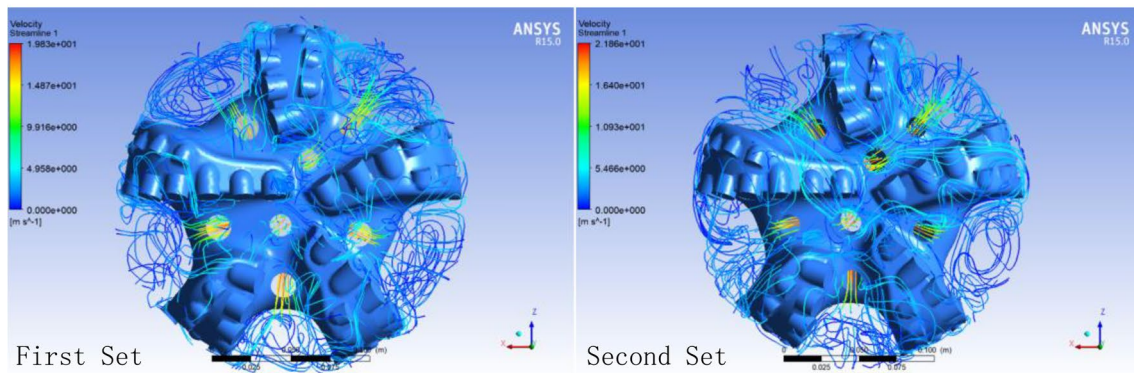
**(b)** Contrast cloud map of the flow field coverage area
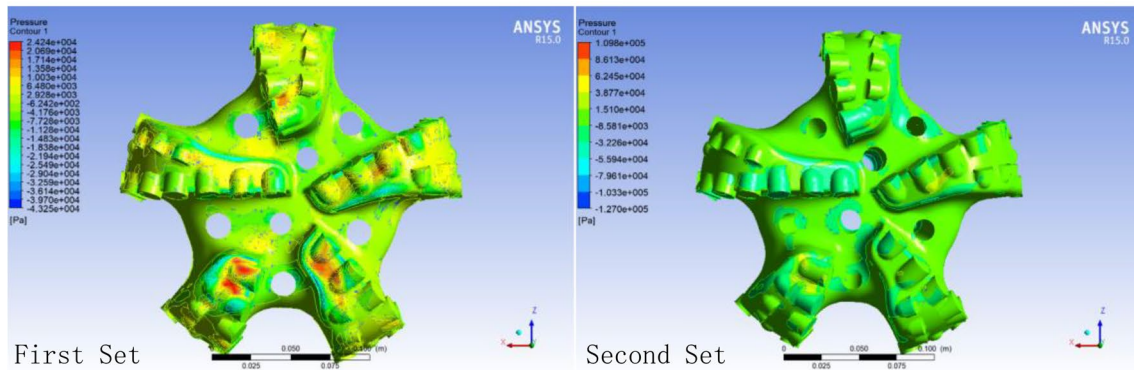
(c) Contrast cloud map of the stress field on the surface of the drill bit

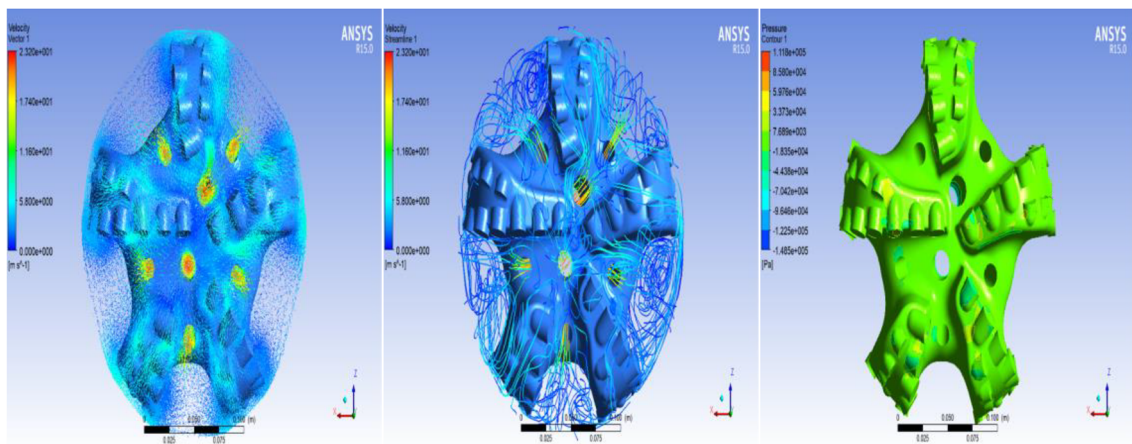**Fig. 10** Comparison of the simulation results of the first and second sets of drill bit spray sets

ting in, leaving, and cutting occur. The impact stress concentration generated by this motion causes chipping of the cutting teeth. The cylindrical anti-impact component can be ejected by the spring after the drill bit leaves the rock. After the drill bit is lowered, the cylindrical component first contacts the formation, which effectively reduces the impact force of the rock on the cutting teeth. When the cutter teeth cut into the rock, the circular component retracts a certain length to meet

the cutting needs. The arrangement of this component reduces the possibility of cutting tooth cracks, reduces the wear of the drill bit, and extends the life of the entire drill bit.
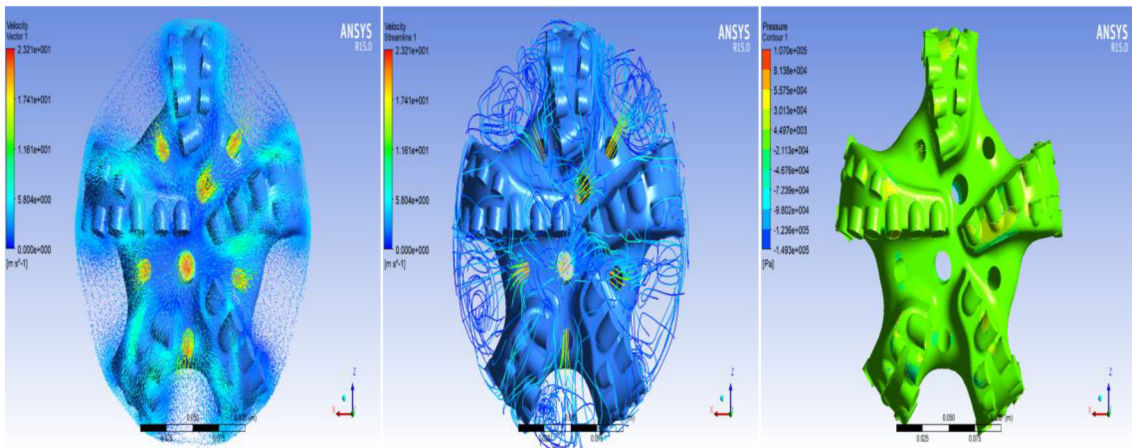
(3) The curved nozzle hydraulic structure is adopted, and the nozzle orientation is set according to the design concept of the rock cutting volume and ensuring cooling and lubrication of the entire drill bit flow field. The curved nozzle hydraulic structure can weaken the
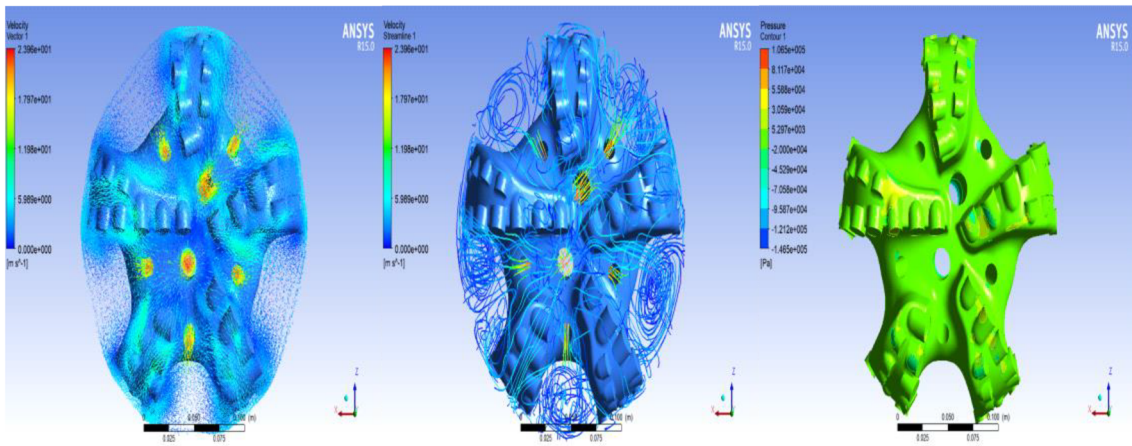
(a) Third set of simulation results

(b) Fourth set of simulation results

(c) Fifth set of simulation results

Fig. 11 Distribution cloud map of the flow field and stress field of the drill bit under three groups of different spray group size combinations

Table 4 Comparison of drill bit usage

Bit size (mm)	Bit symbol	Well depth (m)	Bit drilling depth (m)	Drilling rate (m/h)
215.9	Optimized bit	4036–4298	262 (48 h)	5.46
215.9	MD517X	4298–4432	134 (54 h)	2.46
215.9	SMD517X	4432–4530	98 (34 h)	2.86
215.9	SMD517X	4530–4635	105 (32 h)	3.26

direct impact of drilling fluid on the formation. (Kinetic energy is converted into pressure energy.) The high-speed characteristics of the drilling fluid after flowing out of the nozzle are greatly retained so that the drilling fluid still has a large kinetic energy when it leaves the bottom of the well and has a large flow impact force. It has the effect of high-efficiency cleaning in large-particle and multicutting formations, preventing repeated wear of the vortex of the drill bit by cuttings at the bottom of the well, so it has the characteristics of high-efficiency cleaning.

(4) On the side blades of the bit, gauge teeth are arranged to prevent problems such as a stuck drill and diameter reduction so that the bit is not worn by rocks on the side.

(5) The entire drill bit structure follows the principle of stress balance, the flow field design of the diversion groove distributes the flow according to the amount of rock cutting, and the PDC cutting gear arrangement follows the principle of light and sealed and covering the entire bottom of the well.

Field application

In view of the characteristics of deep formations, and to meet the actual demand for a high deflection rate of horizontal wells, the use of optimized drill bits in the deflection section and horizontal section has an obvious increasing effect, as shown in Table 4.

Compared with the roller bit, the optimized bit can reduce the drilling pressure, reduce the bit jump, and improve the mechanical drilling speed. Compared with the conventional PDC bit, the bit can improve the ability to drill tight mudstone and hard interlayers, reduce the stick slip of the bit, and improve the stability and directional control of the bit.

Conclusion

In this paper, the fracture pattern of deep complex rock strata in the Jidong Oilfield is analyzed. Combined with the shortcomings of existing drill bits, the optimization scheme of personalized drill bits is proposed. The following conclusions are obtained:

(1) The soft-hard interlacing and poor drillability of deep rocks in the Jidong Oilfield lead to low rock breaking efficiency. The formation drilling resistance profile, which can directly assess the rock hardness, drillability, shale content, and lithology distribution corresponding to the depth of a well, is established.

(2) Mechanical analysis of PDC broken rock is carried out. When the back angle of the bit cutting tooth is designed to be 15°, a larger stress concentration range is generated, and the rock crushing efficiency is the highest at this time.

(3) It is most reasonable to design two 16-mm central nozzles and five 14-mm peripheral nozzles. Finally, the overall optimization scheme of the drill bit is proposed, which has an obvious effect on timely improvement in field applications.

References

Li W, Zhao D, Tao F, Lv Z, Li N, Zhao X (2021) Analysis and application of optimal and fast drilling technology in gaoshangpu block of Jidong Oilfield. IOP Conf Ser Earth Environ Sci 791(1):012143

Arsentiev YA, Soloviev NV, Nazarov AP et al (2018) Effect of PDC cutter rake on penetration rate of wing bit drilling in variable hardness rocks. Gornyi Zhurnal 11:47–50

Checkina OG, Goryacheva IG, Krasnik VG (1996) The model for tool wear in rock cutting. Wear 198(1–2):33–38

Chen Y (2008) Experimental study of rock-breaking with an offset single cone bit. Pet Sci 5(2):179–182

Geoffroy H, Minh DN (1997) Study on interaction between rocks and worn PDC'S cutter. Int J Rock Mech Min Sci 34(3–4):611–611

Haimin Z, Xuejun C, Jianming H et al (2006) Horizontal well development technique and its practice for complex fault-block reservoirs in Jidong Oilfield. Pet Explor Dev 33(005):622–629

Ji Z, Shi H, Dai X et al (2021) Fragmentation characteristics of rocks under indentation by a single PDC cutter. J Energy Resour Technol 143(10):1–13

Kuang Y, Zhang M, Feng M et al (2016) Simulation and experimental research of PDC bit cutting rock. J Fail Anal Prev 16(6):1–7

Liu B, Cao X, Ji S et al (2018) Simulation and experimental research on flow field and temperature field of diamond impregnated drill bit. Jingangshi Yu Moliao Moju Gongcheng/diam Abras Eng 38(5):33–38

Sinor LA, Powers JR, Warren TM (1998) The effect of PDC cutter density, back rake, size, and speed on performance[C]//IADC/SPE drilling conference. OnePetro

Tie YAN, Rui XU, Wenfeng SUN et al (2021) Similarity evaluation of stratum anti-drilling ability and a new method of drill bit selection. Pet Explor Dev 48(02):450–459

Wang B (2019) Experimental study on rock fragmentation efficiency of two stage PDC bit. Sci Discov 7(2):92

Wang NC, Zhao JZ, Ding WL et al (2015) Development characteristics of shale fracture in longmaxi formation in southeasten Sichuan. Nat Gas Geosci 10(4):354–354

Wang C, Li S, Zhang L (2019) Evaluation of rock abrasiveness class based on the wear mechanisms of PDC cutters. J Petrol Sci Eng 174:959–967

Wangde Q, Guojun W, Haojie L (2021) Formation drillability prediction by using cascade model based on well logging data in the deep drilling process. Petroleum. https://doi.org/10.1016/j.petlm.2021.04.006

Xisheng Lu (2009) High-speed drilling technology for well Gao 17–19 in Jidong Oilfield. Drill Prod Technol 32(01):104–105

Yahiaoui M, Gerbaud L, Paris JY et al (2013) A study on PDC drill bits quality. Wear 298–299:32–41

Yang Y, Zou D, Sun W et al (2012) A swirling jet from a nozzle with tangential inlets and its characteristics in breaking-up rocks. Pet Sci 01:53–58

Zhenquan W, Dongyu S (2014) Optimal design of the flow field of bi-center bit. Proc Eng 73:345–351

Wang Z, Meng J, Zhang Z (2006) Application of acoustic travel time logging in rock drillability prediction. Pet Geol OilField Dev Daqing 25:94–96

Zhou Y, Song W, Cheng D et al (2019) Customized design of micro-core PDC bit and its application in the deep formations of Nanpu Oilfield. Oil Drill Prod Technol 41(02):165–169